ASE-1946

DESIGN, DEVELOPMENT AND EXPERIMENTAL VERIFICATION OF ATOMIC BEAM APPARATUS

INTERIM SCIENTIFIC

CONTRACT NO. NAS 12-143

PERIOD: 15 JULY 1967 THROUGH 30 APRIL 1968

PREPARED FOR

KI / INSTRUMENTATION LABORATORY

NATIONAL AERONAUTICS AND SPACE ADMINISTRATION

ELECTRONIC RESEARCH CENTER

575 TECHNOLOGY SQUARE

CAMBRIDGE, MASSACHUSETTS 02139

18 JUNE 1968

AMERICAN SCIENCE AND ENGINEERING

11 Carleton Street, Cambridge, Massachusetts 02142

ASE

ASE-1946

Design, Development and Experimental Verification of Atomic Beam Apparatus

Interim Scientific
Contract No. NAS 12-143

Period: 15 July 1967 through 30 April 1968

Prepared By

American Science and Engineering, Inc.
11 Carleton Street
Cambridge, Massachusetts 02142

Prepared For

KI / Instrumentation Laboratory
National Aeronautics and Space Administration
Electronic Research Center
575 Technology Square
Cambridge, Massachusetts 02139

Contract Monitor: Dr. Longmire

18 June 1968

CONTENTS

CONTENTS (Cont'd)

ILLUSTRATIONS

ABSTRACT

An apparatus is under construction to measure the optical radiation produced when beams of ionized particles collide with gas phase neutral molecules or atoms at meteoric velocities. The apparatus is described up to its present stage of development, with test results presented for A^+ and Fe^+ ion beams. The system design for the case of $Fe^+ \rightarrow N_2$ is discussed in detail, as is the proposed operating procedure for determining the absolute emission cross-sections. These measurements will be started within the next two months, and will be followed by measurements of the emission of radiation in $N_2^+ \rightarrow Ca$ collisions.

1.0 INTRODUCTION

The visible radiation observed when a meteor penetrates the atmosphere consists almost entirely of atomic and molecular spectra, and is apparently produced at some separation from the meteor's surface. The conclusion is that the mechanisms principally responsible for the observed light and ionization trails are various types of collisions between atmospheric gases and particles either evaporated or rebounding from the surface. Depending on the meteor speed (10 - 70 km/sec) and the particle mass, the interaction energies lie in an approximate range 10 eV to 2000 eV. In order to evaluate the relative importance of the various collision processes, it is necessary to know the pertinent cross sections over the above energy range. Laboratory measurements of these cross sections would not only enhance our knowledge of meteor dynamics, through proper interpretation of the energy transfer processes responsible for the observed light and ionization, but would also add to our knowledge of the physics of atomic and molecular interactions.

The goal of the work being performed under Contract NAS 12-143 is to develop an apparatus and to measure the cross sections for several important processes pertinent to the problem of meteor dynamics. In particular, it is to provide data for the evaluation of emission cross sections for the major spectral features produced in $Fe^{+} \rightarrow N_2$ collisions at meteoric velocities, and to perform preliminary measurements for the case of $N_2^{+} \rightarrow Ca$. The term "emission" cross section is used because the observed radiation may be the result of a cascade process as well as direct excitation. Although atmospheric absorption prevents the observation of meteor spectra in the IR or UV, important processes may occur and it is desirable to extend the laboratory measurements as far as practicable into these regions. The selection of optical components, which will be discussed later, limits the spectral range which will be measured to 1800 Å to 1.0μ.

A schematic diagram of the apparatus is shown in Figure 1. Development of the initial stages of the apparatus was described in the first Interim Scientific Report for Contract No. NAS 12-143, dated 1 August 1967. To study all significant meteor processes, the experimental apparatus is being designed and constructed for two main categories of experiments: (1) neutral-neutral collisions, and (2) ion-neutral collisions. At the time of the first report, the apparatus was essentially completed from the ion source through the mass analyzer and drift-tube, and some design effort for the retarding lens had been done. While continuing the design of a charge exchange chamber necessary for experiments of category (1), it was decided, on the basis of a literature survey and calculations of meteor collision dynamics at NASA-ERC, to investigate processes in category (2) first. This report gives an account of the design and construction of a collision chamber and accessories, for this purpose.

The present state of the apparatus is indicated in the figure. The collision chamber itself is an aluminum cylinder inserted through the experimental region, and equipped with ports at both ends. The experimental region is a vacuum housing of square cross section, mounted horizontally, and attached to the drift-tube exit flange by a flexible bellows coupling, which also contains the retarding lens. The experimental region has been designed with enough volume to allow a charge exchange chamber for producing atomic beams to be inserted between the retarding lens and the collision chamber in the future. An adapter for attaching a vacuum monochromator above the collision chamber completes the vacuum system. The entire apparatus (apart from power supplies, electronics, and auxiliary vacuum system) is supported by the mounting platform, which also serves as a terminus for electrical power and water distribution.

Following a brief review of the early stages, this report describes the remainder of the apparatus up to its present form, including test results. Plans for the proposed experiments are discussed.

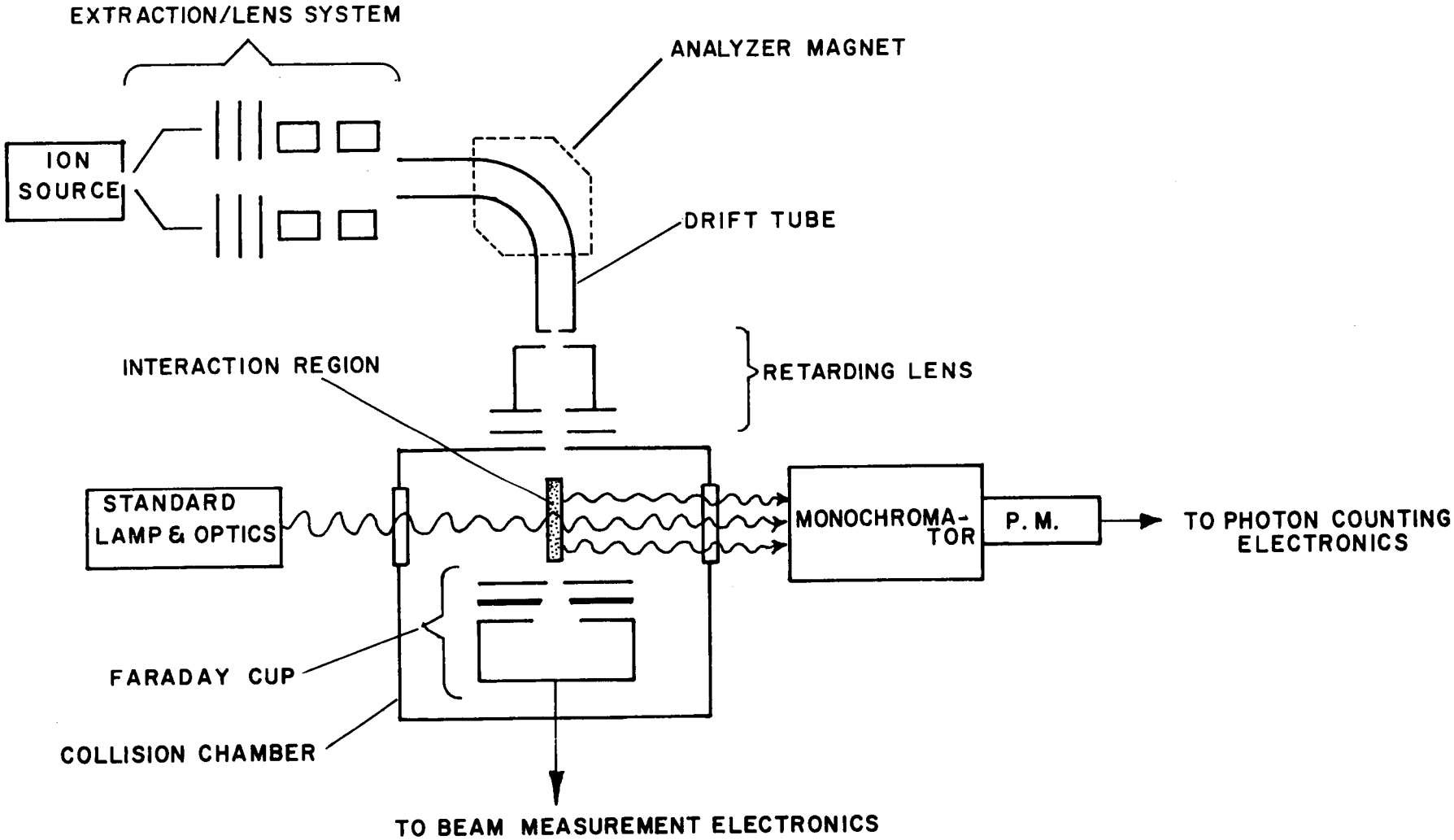

Figure 1 Schematic Diagram: $Fe^{+} \rightarrow N_2$ Experiment

2.0 ION BEAM FORMATION AND CONTROL

In order to obtain a beam of ions of a given species, traveling at meteoric velocities, it is necessary to form a beam of partially ionized gas from which ions may be extracted, to focus the extracted particles into a controllable beam, to filter it for the desired mass, and to adjust it to the desired energy. One other feature is frequently a desirable characteristic of an atomic or ionic beam; that it be modulated, so that selective detection methods can be employed to extract a beam induced signal from noise and background. These features cover the extent of the ion dynamics in the apparatus described, and will be discussed in this section. Figure 2 illustrates the electrical arrangement for this phase of the apparatus.

2.1 Review of Earlier Work

The ion source itself is essentially as descirbed in the first Interim Scientific Report, except for changes made in materials, heating arrangement and radiation shields to enable higher operating temperatures to be used. It is of the Nielsen type, (Reference 1) and is arranged in such a way that the discharge chamber can be operated at a high potential relative to ground.

The beam is extracted through the 1.5 mm diameter source aperture by a conical extraction electrode which accelerates the ions to a nominal energy of 2000 eV. This electrode is followed by a three-element einzel lens and two electrostatic quadrupoles. The effect of this array is to shape the beam into a rectangular cross section (approximately 10 mm high x 2 mm wide) at the object plane of a 90° sector magnetic analyzer. An electroformed copper drift-tube, whose entrance and exit apertures coincide with the analyzer object and image planes, provides for vacuum integrity through the magnet pole gap. This design allows easy installation of limiting slits at either plane to reduce aberrations and improve the mass selection.

The ion source and lens operating parameters were investigated

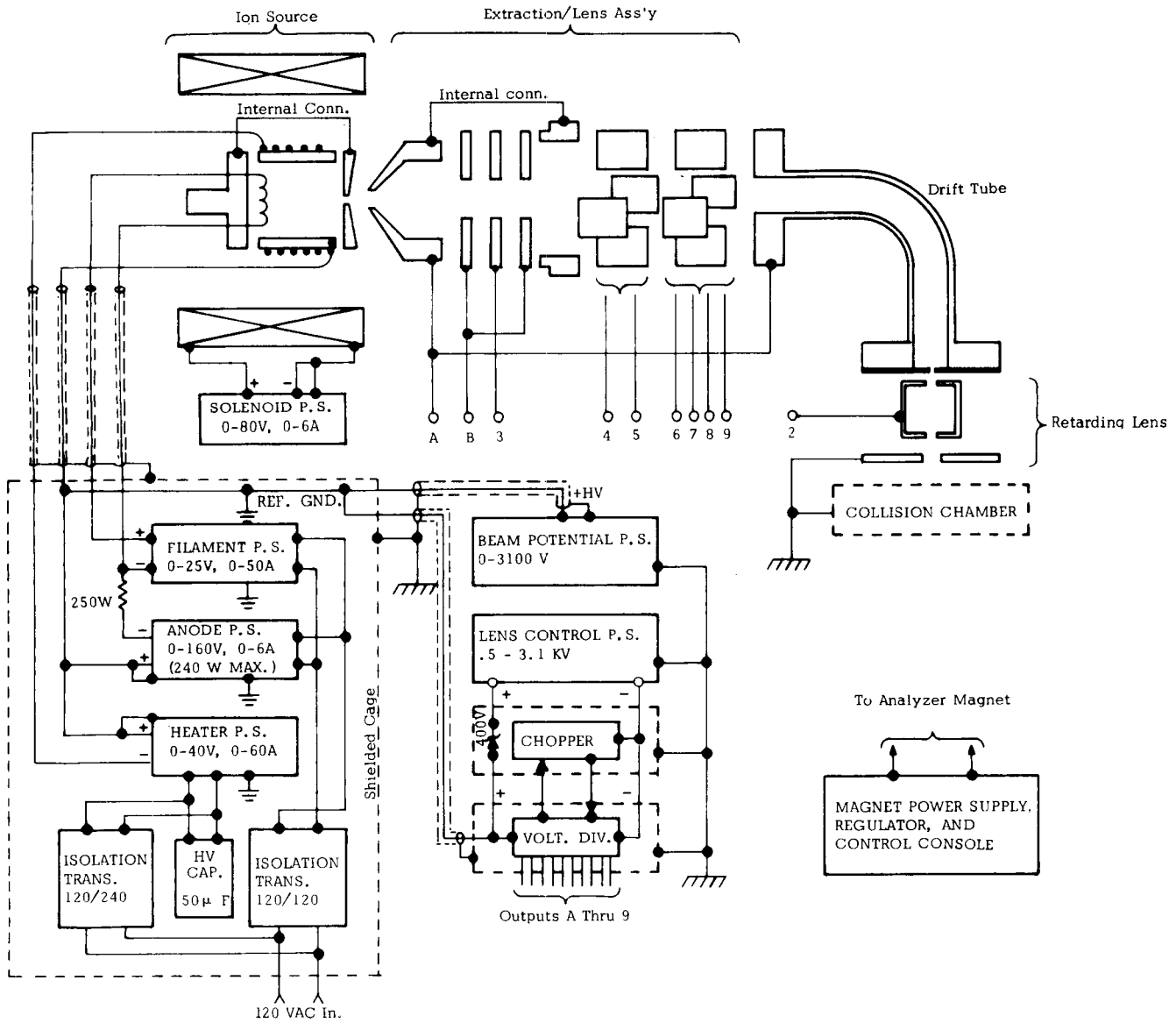

VOLTAGE DIVIDER OUTPUTS*

A EXTRACTION: .8 Tap Direct

B MODULATION: Chopped Between .8 Tap & 400V Stopping Potential

2 RET. LENS: .5 to 1.0 in 0.1 steps

3 EINZEL: .2 to 1.0 Continuous

4 1st Quad., Horiz.: .5 to 1.0 Continuous

5 1st Quad., Vert.: .5 to 1.0 Continuous

6 2nd Quad., Left: .5 to 1.0 Continuous

7 2nd Quad., Right: .5 to 1.0 Continuous

8 2nd Quad., Up: .5 to 1.0 Continuous

9 2nd Quad., Down: .5 to 1.0 Continuous

*Fraction of Input Voltage Measured From Reference Ground.

Figure 2 Schematic Diagram: Ion Beam Formation And Control

and discussed in the earlier report. Lens control was accomplished by simply providing a separate power supply for each desired potential. This system was unwieldy, and has since been replaced with a single power supply and a voltage divider control network. Beam measurements were made with a multiple-element detector array, which was moveable along the beam axis. (The same arrangement has been used for ion beam studies at the output of the magnetic analyzer and the retarding lens, to be descirbed later in this section.) A summary of the previously reported ion source and lens studies follows:

The basic parameters affecting the ion source and lens operation are filament emission, anode voltage, axial magnetic field, discharge pressure in the plasma (determined by the chamber temperature or the leak valve setting, depending on the beam material), extraction gap, extraction voltage, and lens electrode potentials. In addition, there is provision for rotation of the lens about its longitudinal axis to align the beam image. The plasma could be started with any emission current greater than 1 ma (anode voltage set at 75 v) by proper adjustment of the gas flow and axial field. The plasma current was limited to 2 amps by the power supply. High anode voltage and high axial field (2 - 3 amps through the solenoid) were observed to maximize the plasma current, although these depended on the gas flow setting.

The focused beam current did not maximize with the same settings as the plasma current. Of a total beam current of 25 ma, 4 - 7 ma could be focused through a 10 mm x 2 mm slit at the design focus. This value peaked at the minimum axial field and gas flow rate for which a plasma could be maintained.

The parameters affecting ion source and lens operation were observed to be greatly interdependent, so an iterative adjustment technique was most successful in maximizing the beam. It was also clear that the

power supplies providing the lens potentials were inadequate, and that higher voltages were needed.

2.2 Present System Configuration

2.2.1 Ion Source Modification

To operate the ion source on a plasma of iron vapor, or any of several other low vapor-pressure meteoric constituents (Ni, Si, Ca), requires that temperatures up to about 1500°C be produced and sustained inside the discharge chamber. To achieve this aim, and to provide independent control of the heating and electron emission functions, the dual-filament discharge chamber shown in Figure 3 was constructed. The design minimizes thermal stresses, and all parts subjected to a severe temperature environment are of high-temperature materials: grade HP boron-nitride insulators, graphite electrodes, tungsten or molybdenum filaments, and molybdenum radiation shields.

In operation, the charge material may either be inserted in solid form, leaked in as a gas, or retained in a boron-nitrate or graphite crucible. The temperature may be controlled by the external heater, while the plasma is initiated and sustained by electron emission from the small central filament. The four cylindrical heat shields and the disc substantially reduce the power required to heat the source. To run an iron beam, a total power input of about 300 watts is required, of which about 100 watts are supplied by the emission filament.

The wiring diagram for the modified ion source is included in Figure 2. This is somewhat different than that shown in the first Interim Scientific Report, since an extra power supply is needed for the heater. A new anode supply provides ample power for the plasma current (up to 160 v or 6 A, with a maximum power output of 240 W).

Operating characteristics for the modified ion source are

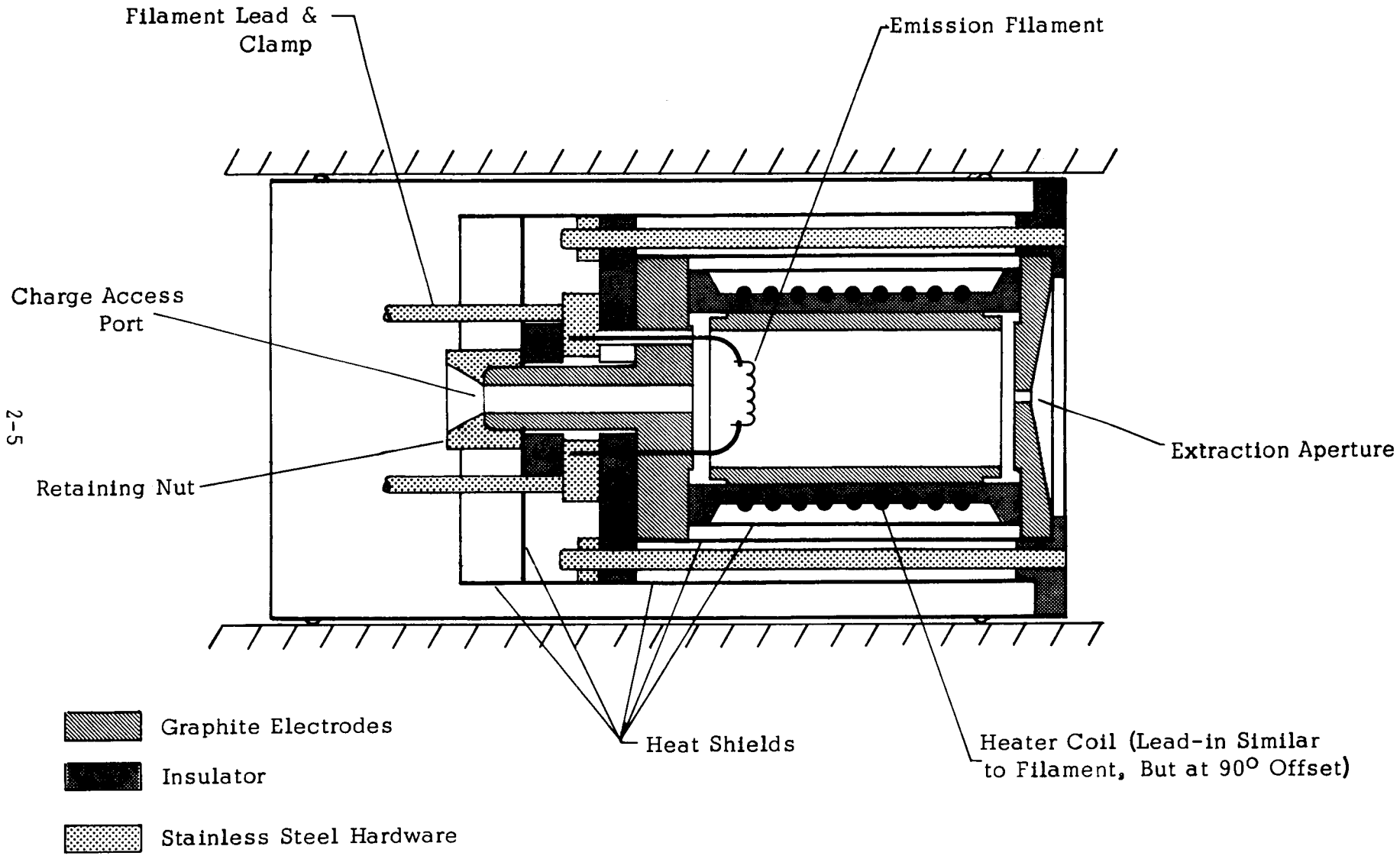

Figure 3 Ion Source Assembly

essentially the same as those described earlier. The basic parameters of operation have not been changed.

2.2.2 Extraction and Focusing

Rather than continue with the multiple power supply arrangement to control the extraction and focusing of the ion beam, it was desired to obtain the lens potentials from a single power supply by means of a voltage divider network. A ten-stage transistor chain divider was designed and built expressly for this purpose by Northeast Scientific Corporation. It divides the input voltage into ten equal increments, from which the desired voltages may be obtained either directly, or by switching a ten-turn potentiometer across two adjacent taps and adjusting the potentiometer for fine control. Figure 4 illustrates the basic stage of the divider chain and indicates how the outputs are obtained.

The advantage of a transistor voltage divider over a purely resistive one is that it can provide a number of independent outputs from a single, regulated chain, thus giving better stability with lower power dissipation. Unfortunately, the unit is a prototype and has been susceptible to damage by accidental short circuits or high voltage transients. Protective circuits have been added in an attempt to prevent further breakdown, but only continued use will test their success.

The relationship of the voltage divider and its outputs to the rest of the system is shown in Figure 2. It should be noted that the divider receives its input voltage either directly from the Lens Control Power Supply, or with a 400 v drop through the chopper. The above three units (housed within grounded cases) float at a potential above ground, determined by the Beam Potential Power Supply. This allows the beam to be extracted, focused and mass analyzed at a fixed energy (nominally 2 keV), then retarded to an energy established directly by the Beam Potential Power Supply. All collision measurements may therefore be done at ground potential, and only

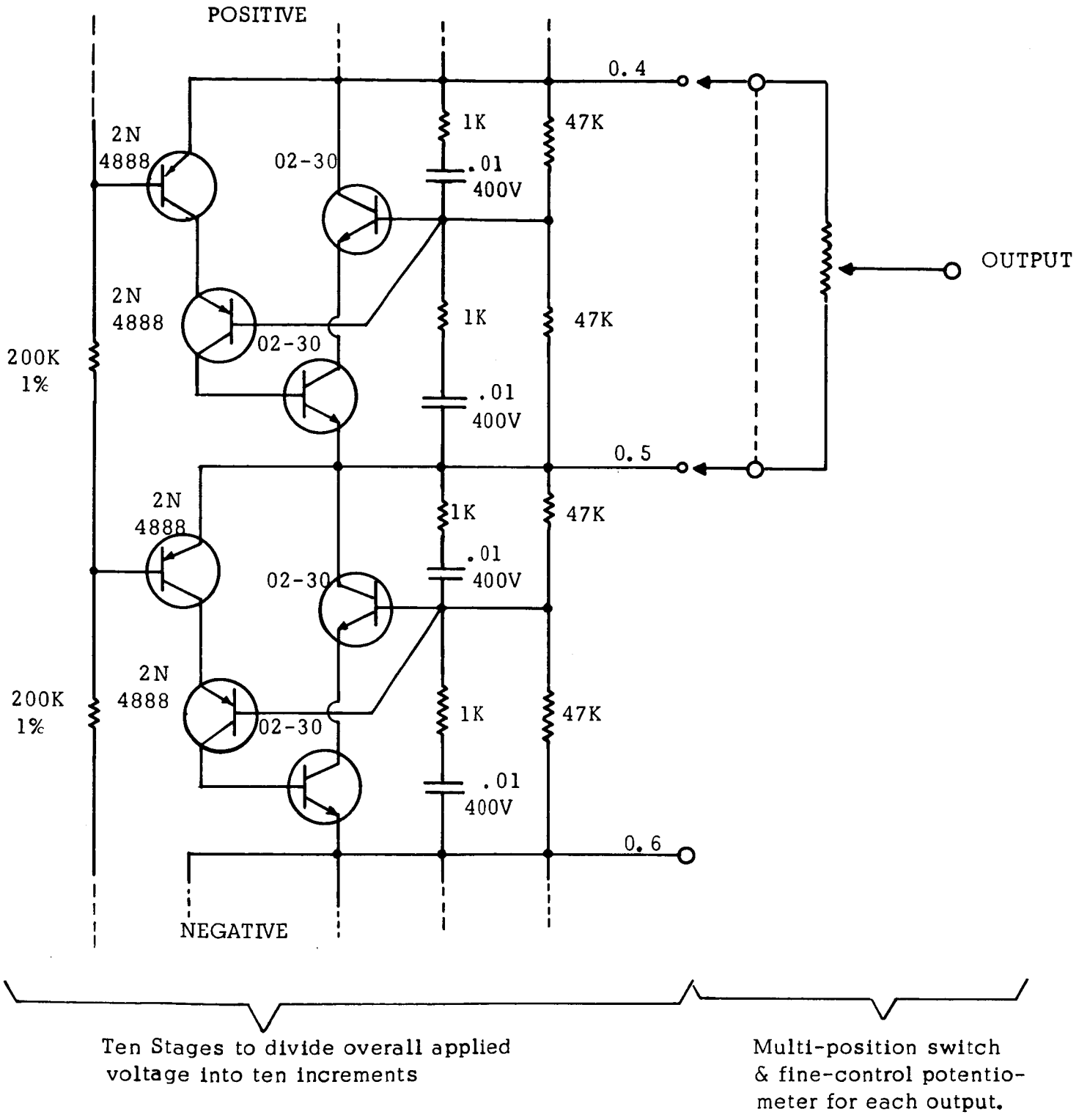

Figure 4 Voltage Divider Chain

one voltage must be changed to alter the collision energy.

2.2.3 Mass Analysis

Design and construction of the mass analysis region was described in the earlier Interim Scientific Report; the only changes made since then have been the addition of teflon insulating material around the drift-tube, and installation of a magnetic shield (sandwiched Netic and Co-netic sheets). The latter also creates a physical barrier to prevent personnel from contacting the drift-tube, which may be at high voltage during beam operation. Results of operational tests and measurements will be given later.

2.2.4 Beam Retardation

The final ion energy is determined by the net potential drop between the plasma in which the ions are formed and the grounded collision chamber. The potential distribution in a plasma discharge is such that the plasma boundary is within a few volts of the anode potential, the difference being called the "anode fall" (References 2 & 3). Positive ions extracted from the plasma may therefore be assumed to originate essentially at anode potential. Again referring to Figure 2, we see that this is established by the Beam Potential Power Supply, the output of which is a common reference potential for all other ion source and lens voltages.

The function of the retarding lens is to provide some means of control over the beam trajectory as it is decelerated between the exit apertures of the drift-tube, where it has the energy imparted to it by the anode-extraction electrode potential drop, and the entrance to the grounded collision region. The geometry used is shown in Figure 5. Deceleration takes place in two stages: the first is between the drift-tube exit slit and the entrance of a field free cylinder, the second between the cylinder and an apertured plate at ground potential. The potential of the field-free region is set by one of the voltage divider outputs. It is adjusted for best focusing

and collimation of the beam as measured by a Faraday collector in the collision region. The action of this retarding lens is very similar in principal to that described by Neff (Reference 4) except that his field-free region was maintained at the final beam potential, and served as the first element of an einzel-lens array for the beam focusing (see Figure 5).

2.2.5 Beam Modulation

It was mentioned in the introduction to this section that modulation or chopping of the ion beam is a desired feature. Since we are dealing with a beam of charged particles, it seems reasonable to chop the beam by electronic application of periodic defocusing or stopping voltages to the lens system preferably in a square wave-shape. In the first Interim Scientific Report, it was proposed to apply the modulation signal to the center element of the einzel lens, and tests indicated that this was feasible. The potential distribution in a three-aperture einzel lens, such as we have, exhibits a saddle point at the center of the lens (References 5 & 6). In order for the charged particles (positive ions) to be totally reflected, the axial potential at this point must be positive. Reference 6 gives an expression for the critical potential which must be applied to the center lens element for this condition to be satisfied:

$$V_c = - \frac{1}{\frac{Z_o}{R} \tan^{-1}\left(\frac{Z_o}{R}\right)} V_2$$

where V_2 is the potential of the outer electrodes (equal to the incident beam energy),

Z_o is the separation between lens elements, and

R is the radius of the center aperture.

Our geometry and extraction voltage is such that $V_2 = -2$ kV (relative to the plasma), $Z_o = 0.75"$, and $R = 0.25"$, which gives for the critical potential, $V_c \approx 540$ v. Thus, it would be possible to chop the beam by switching the

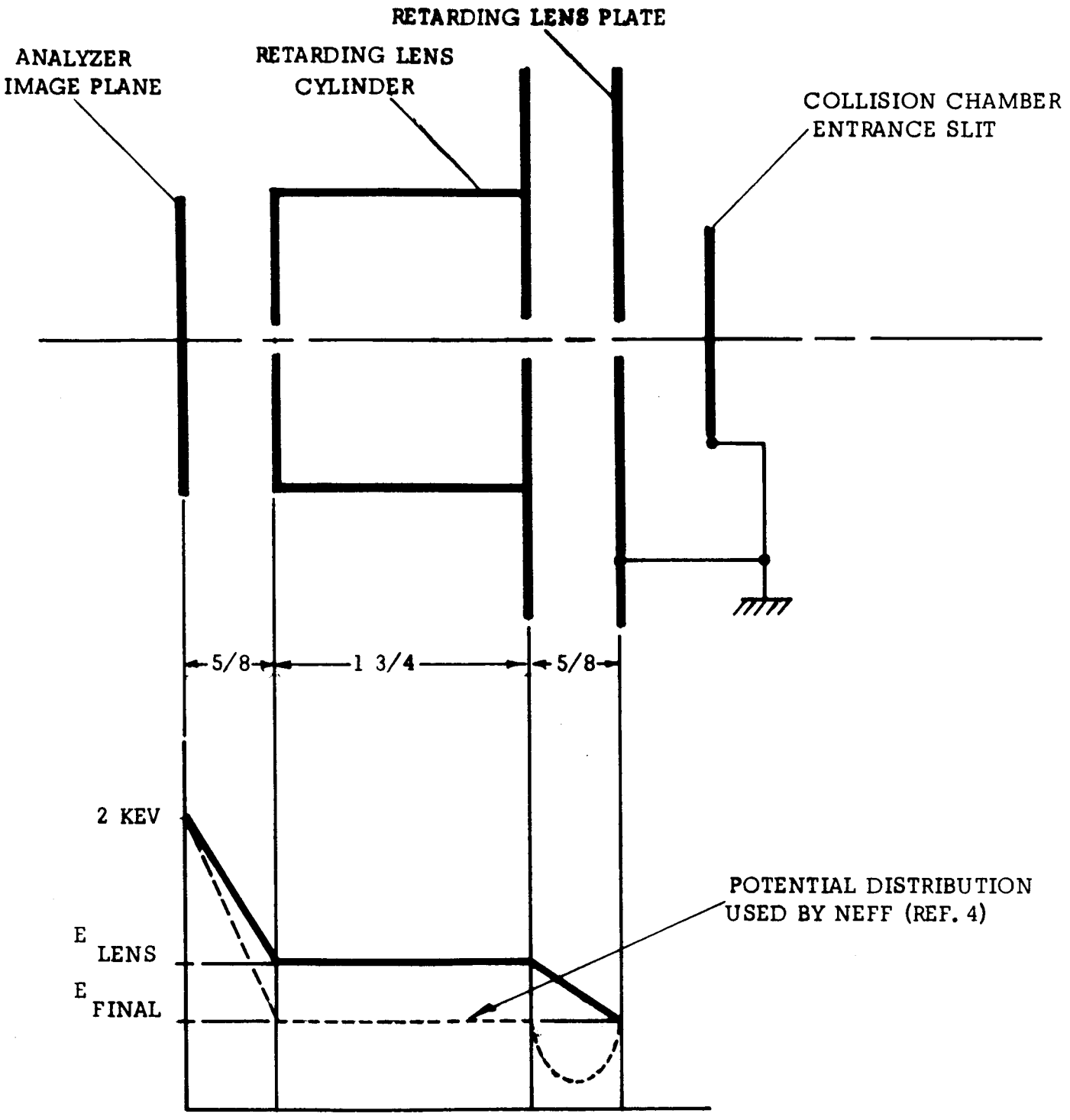

Figure 5 Retarding Lens Geometry and Potential Distribution

center einzel lens electrode between + 540 v (or greater) and the voltage (about - 1000 v) for which the proper focus is achieved, where both voltages are referenced to the plasma. This requires either two power supplies, or the use of a voltage dividing arrangement such as the zener diode shown at the chopper in Figure 2.

It is apparent that a grid across the center aperture would cause the beam to be reflected at a lower repelling voltage. This possibility must be rejected, however, since the transmitting mode potential distribution would be drastically affected (the saddle point would be destroyed), resulting in a negative focal length.

An alternative chopping method, which may be used with or without grids, is to apply the repelling potential to the outer einzel electrodes. Although the critical potential has not been evaluated for this' case, geometrical arguments indicate that even without grids the repelling voltage required is less than for the case described above.

The heart of the chopping circuit is shown in Figure 6. The Lens Control Power Supply output is attached to terminals 1 and 2. Its output minus 400 v (dropped by two 1N3015A zener diodes) is applied to the voltage divider input, terminals 3 and 5. The 0.8 tap from the divider is brought into the chopper circuit at terminal 4. The function of the chopper is to provide an output which alternates in potential between those of terminals 1 and 4, which are reflecting and focusing potentials respectively. This is done by applying a modulation signal A and its complement $\overline{A}$ to the grids of the two tubes T 1 and T 2, so they alternately conduct and turn off. When T 1 conducts, high voltage diode D 1 is forward biased and the output is at the potential of terminal 4. When T 2 is conducting, it drops only a small voltage and the output rises close to terminal 1. In this case D 2 is forward biased and D 1 is cut off. The currents through the tubes are i_1 and i_2 respectively. Typical operating voltages are indicated, measured relative

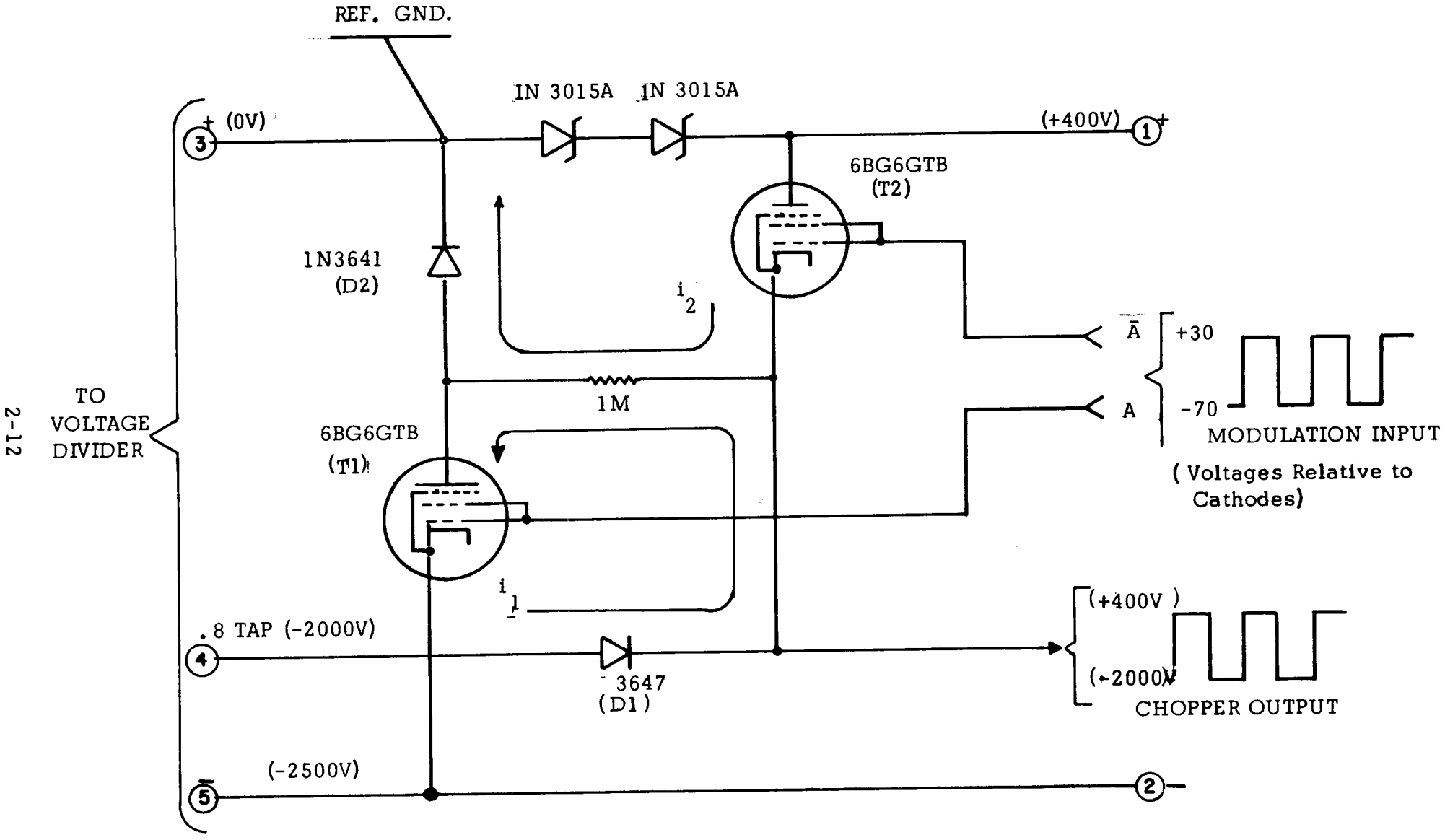

Figure 6 High Voltage Modulator

to the plasma or "reference ground". The circuit shown floats with respect to true earth ground by a voltage determined by the Beam Potential Power Supply (See Figure 2).

2.3 Operational Tests

In order to verify the operation of each stage of the apparatus and to study the system parameters, beam measurements were made as required. The data obtained were used as design inputs for following stages, in accord with the semi-empirical approach adopted at the start of the project. Figure 7 shows the geometry of the test setup and the detector array used for all current measurements. The detector array may be moved along its axis, or rotated about it.

2.3.1 Lens and Magnet Operating Conditions

It was not necessary or possible to make completely independent tests of the magnetic analyzer, since the ion source and lens system were needed to provide an input. Consequently, the three were studied together by means of their effect on the beam behavior. Measured data are illustrated graphically in Figures 8 - 11. Because of the great interplay between the various system parameters, the beam was generally tuned for best characteristics after a particular parameter was set. For example, in studying the properties of the focused beam as a function of solenoid magnet current, the lens and analyzer magnet were retuned each time the solenoid current was changed since we wanted "best" beam vs the parameter.

The conditions under which the data were obtained were: argon gas as the charge material, a 2 keV extraction energy, the original ion source discharge chamber with a U-shaped filament of .040" ta wire, a "home made" voltage divider arrangement with maximum outputs of $\pm$ 350 v, and a fixed anode voltage of 76 v. Operating conditions for each case are

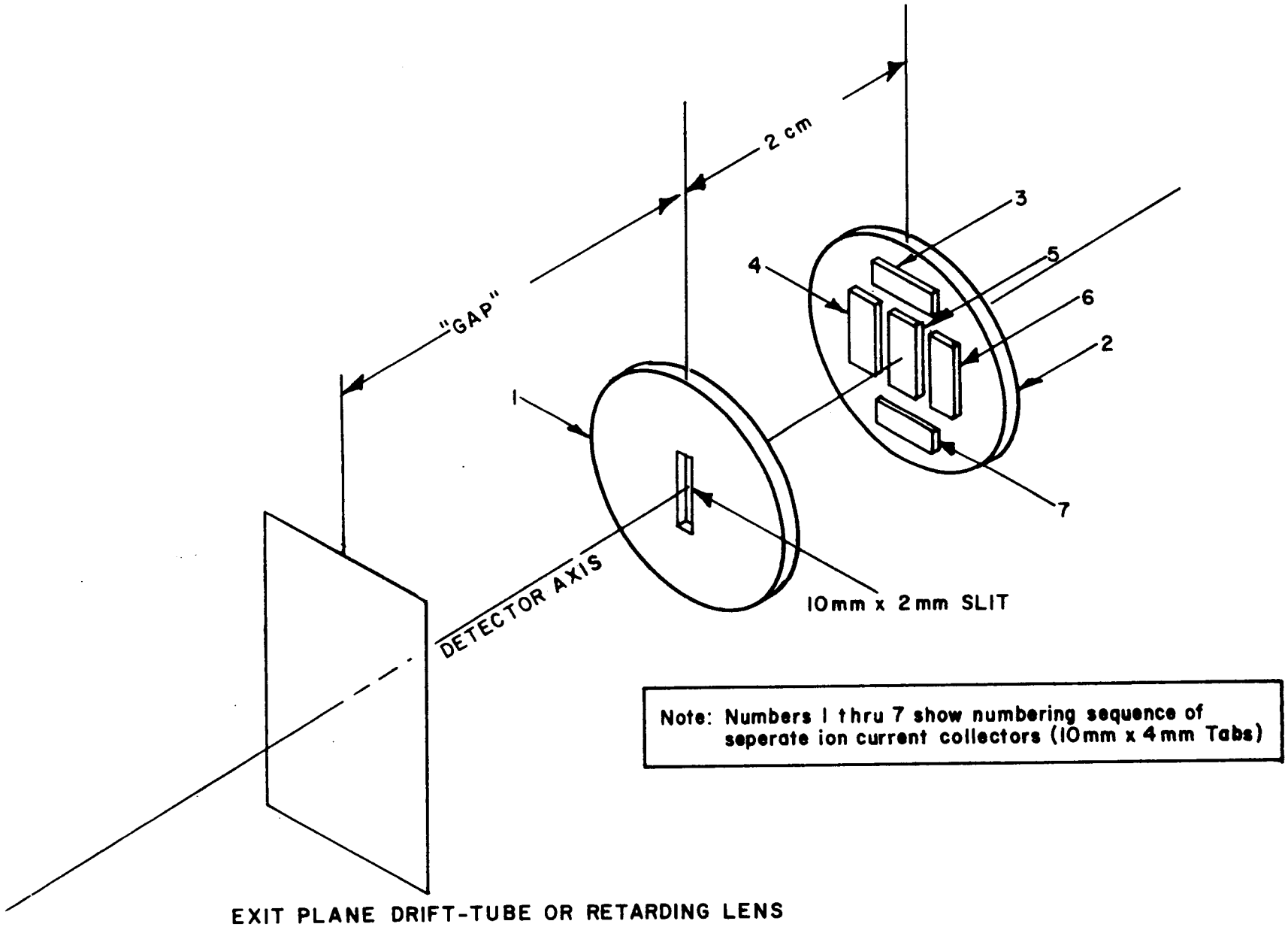

Figure 7 Detector Array Geometry

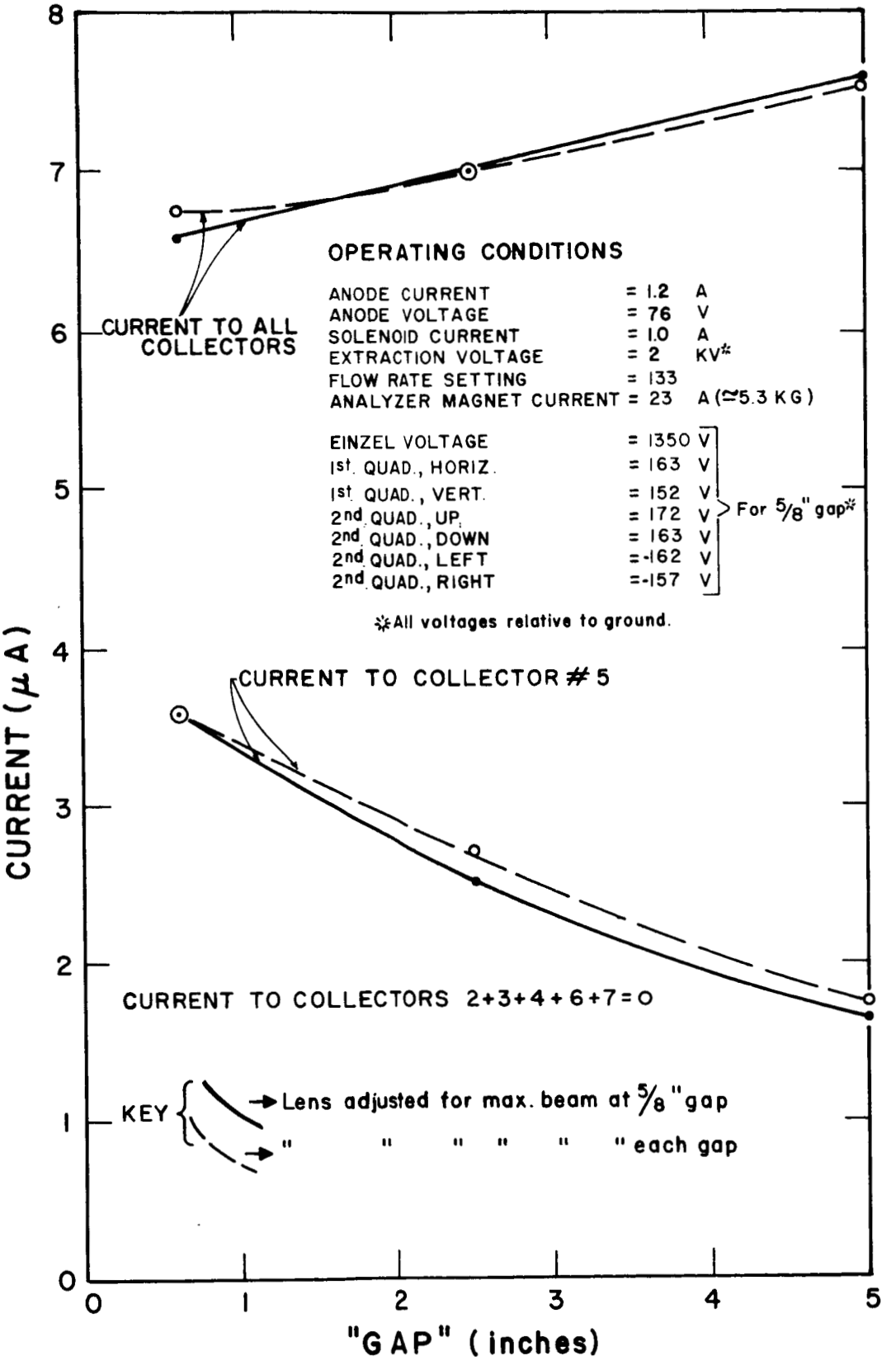

Figure 8 Detector Current Vs "GAP"

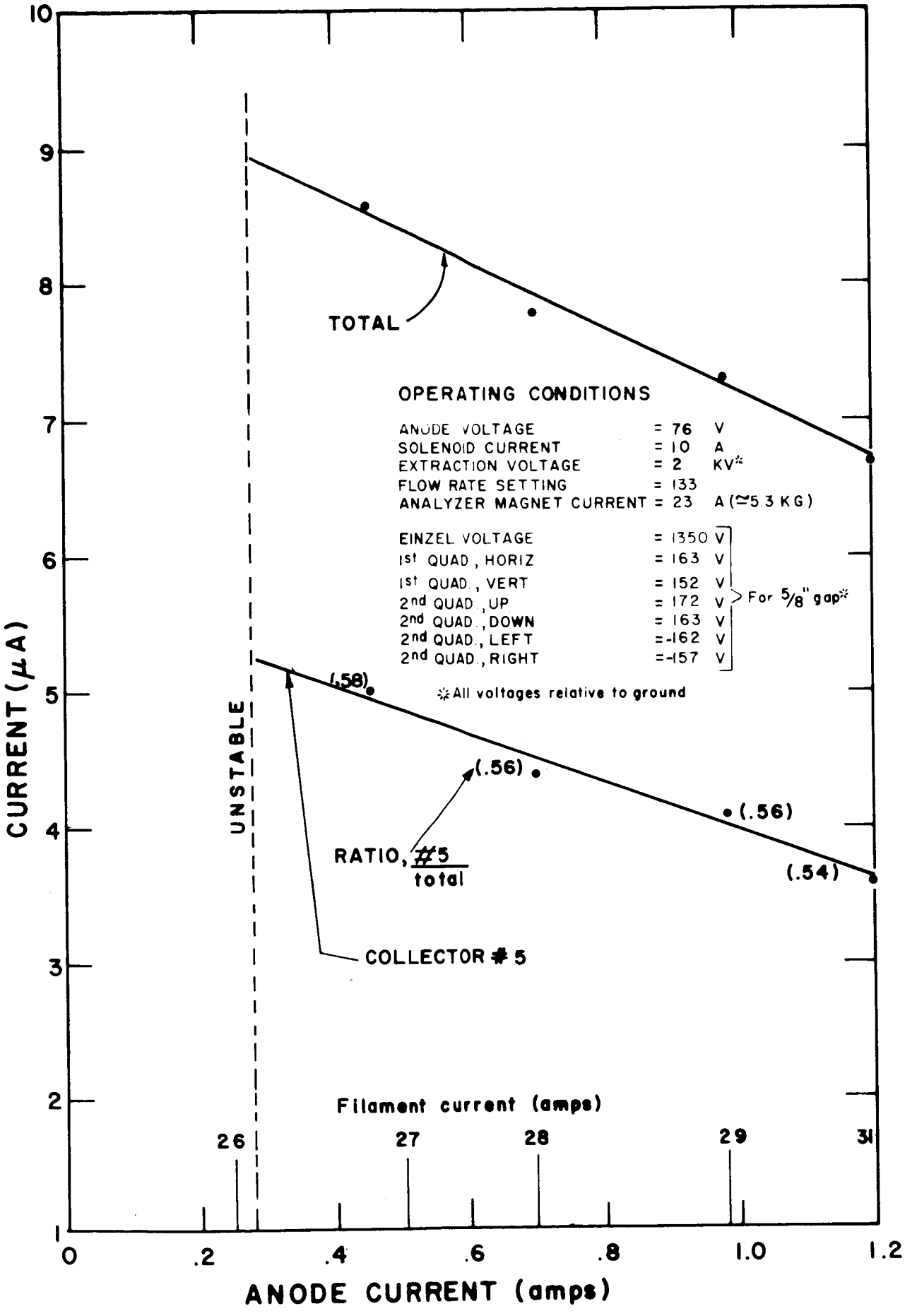

Figure 9 Detector Current Vs Anode Current

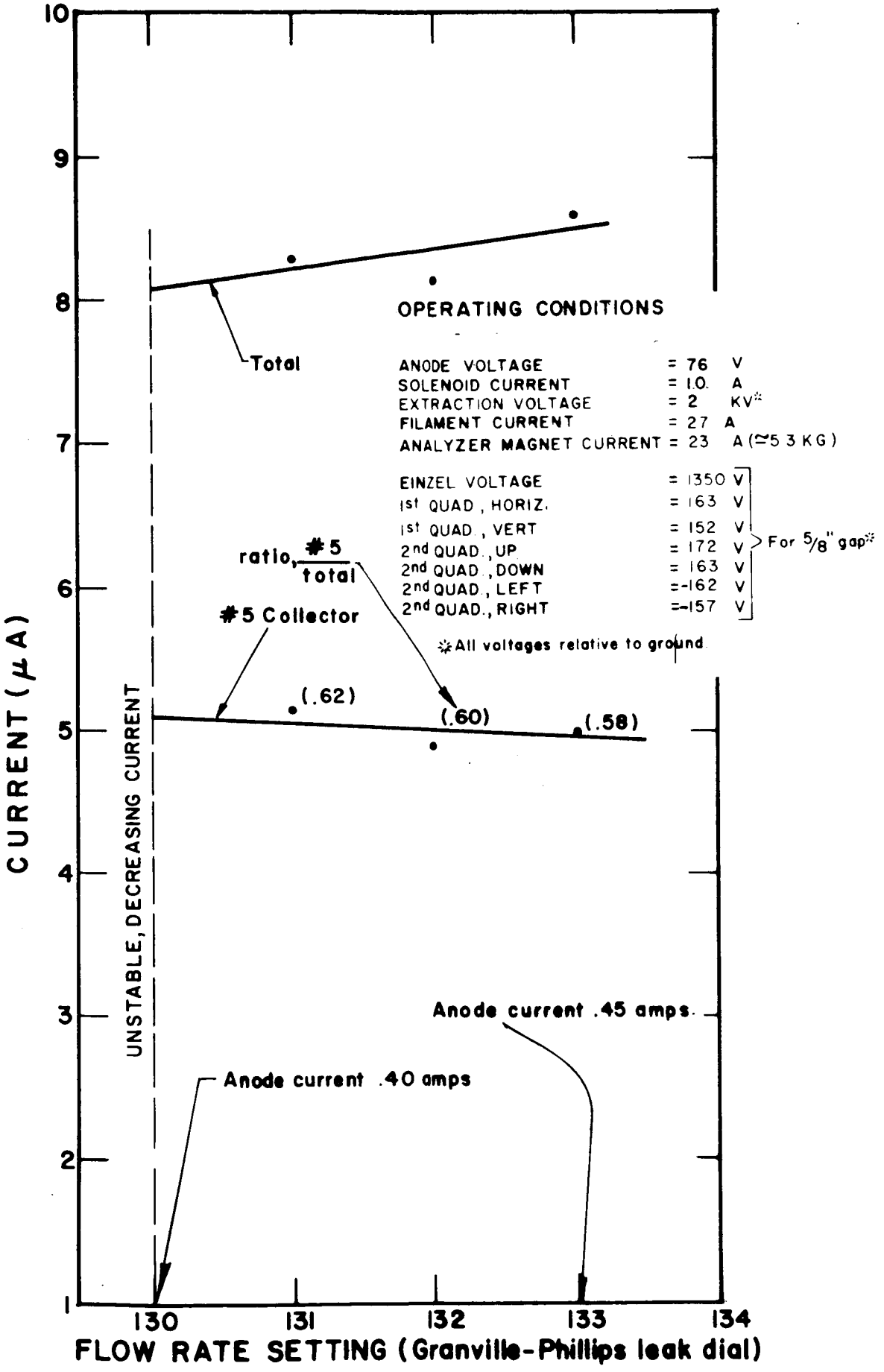

Figure 10 Detector Current Vs Flow Valve

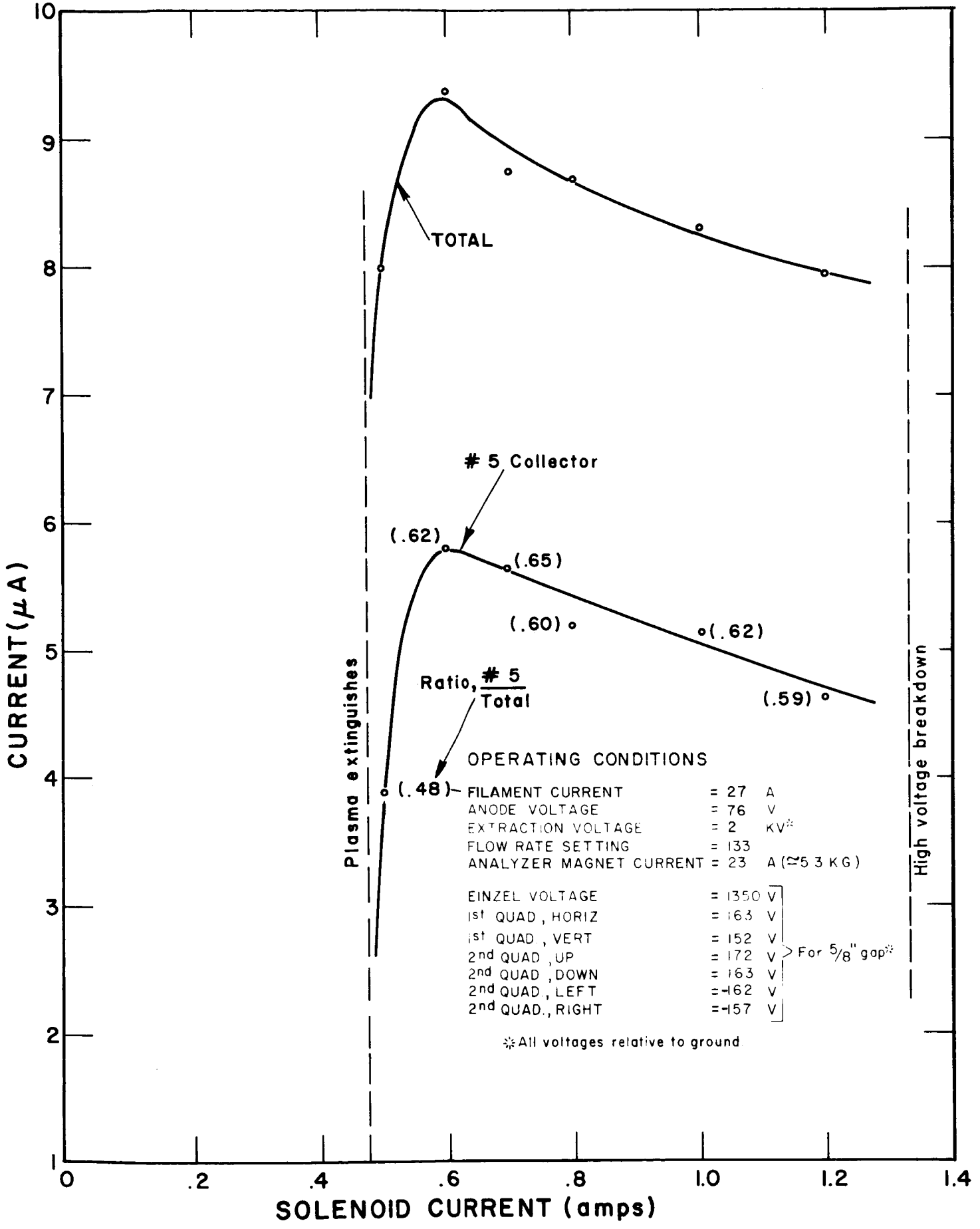

Figure 11 Detector Current Vs Solenoid Current

given on the graphs.

The following general observations may be made:

1. Assuming uniform current density in the beam, the fall-off rate shown in Figure 8 leads to an upper limit of 2° half-angle of divergence; that it is less then 3° (.05 radian) is also confirmed by the fact that all current passing through the slit in detector #1 is collected by tab #5.

2. Focusing conditions for maximum beam do not change much for different "gap" lengths; this is again indicative of the fact that the beam is nearly parallel.

3. Best focused beam current and best beam efficiency are obtained using the minimum anode current, gas flow, and axial magnetic field for which a stable plasma can be maintained.

4. About 60% of the beam can be focused through a 2 mm x 10 mm slit with a divergence less than .05 radians.

5. Beam currents up to 6 μA or more may be obtained for A^{+} at 2000 v extraction potential.

6. The above results and the general nature of the data presented on graphs are consistently reproducible.

2.3.2 Mass Scans and Resolution

By scanning the magnetic field of the mass analyzer so the beam moves across the slit in detector #1, we can get an indication of the mass resolution of the system. The data plotted in Figure 12 represent such a scan. The magnetic field is proportional to the current (neglecting hysteresis and core saturation, which are small for a limited range of scan), and can be related to the ion mass and charge by the equation

$$r = 4.61\sqrt{\frac{M\,V}{q\,B^2}}$$

Figure 12 A^{40+} Mass Scan

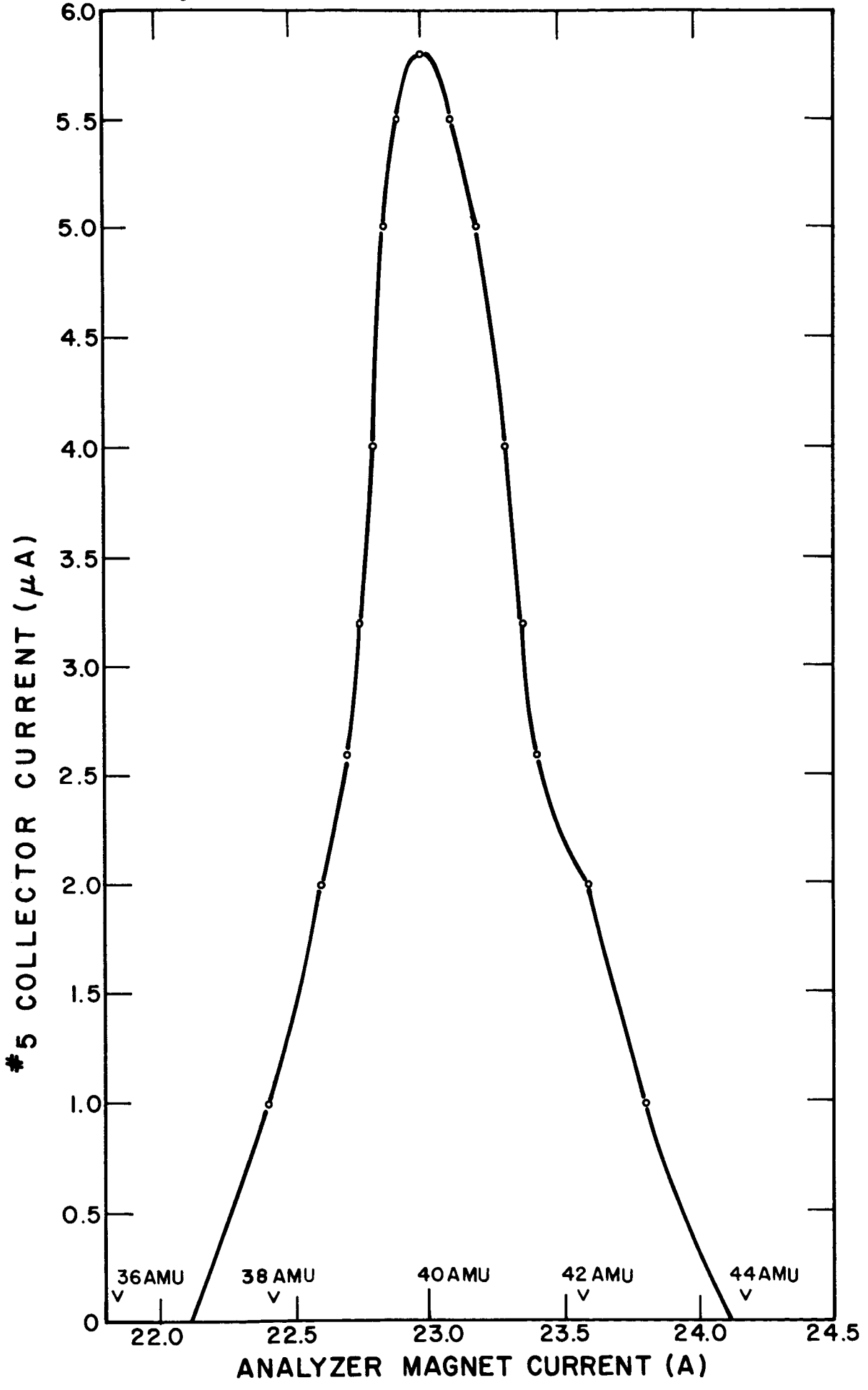

where r = radius of curvature (cm),

q = number of elementary charges carried by ion,

B = magnetic field (kilogauss),

M = particle mass (AMU),

V = energy (keV).

The mass scale is also indicated on the figure. We observe that a similar mass peak centered at 44 AMU would make no appreciable contribution to the A^+ peak at 40 AMU, corresponding to a system resolution of better than $R = 10$. (In mass spectrometry, peaks are considered to be resolved if the intervening valley does not exceed 10% of the sums of the peaks. This is a more stringent requirement, for which the resolution indicated by the plotted scan would be $R \approx 8$.) The above result is only an approximation and may be taken as a lower limit of resolution for the production of an uncontaminated ion beam.

A true measure of the resolution could be obtained by scanning the mass peaks across a slit located at the analyzer focal plane. Such a slit is required in any case in order to limit all but the desired mass from being transmitted through the rest of the system and into the collision chamber. To improve the resolution it is necessary to either provide a sharper focus at the analyzer object plane, or to place a limiting aperture (slit) at that location. Better defined images may then be formed, without having changed the dispersive characteristics of the analyzer.

Complete field scans were also made to see what mass peaks could be observed and identified. Fifteen to twenty peaks were detected, of which the more important are

A^+ (40 AMU), 4.4×10^{-6} A;

A^{++} (40 AMU), 8.0×10^{-7} A;

N_2^+ (28 AMU), 2.4×10^{-8} A'

A^+ (36 AMU), 2.3×10^{-8} A;

CO_2^+ (44 AMU), 1.3×10^{-8} A.

Note that A^{40} and A^{36} were resolved; the natural abundances of these isotopes are in the ratio 320:1.

2.3.3 Retarding Lens Operation

By adjusting the potential applied to the cylindrical element of the retarding lens (see Figure 5) it is possible to control the ion beam focus as its energy is reduced. The moveable detector array was used at the retarding lens output to measure the beam current and focal properties. The beam could be slowed to about 100 eV with little or no loss of intensity. The beam divergence was somewhat affected, however, and depended strongly on the retarding lens setting. For any given energy it was possible to make the beam practically parallel (i.e., independent of "gap"), accompanied by some loss of intensity.

2.3.4 Iron Beam Operation

Iron beams were run on several occasions, with no unexpected difficulties. The procedure used was to start an argon plasma in the usual way, and then gradually increase the power (by means of the heater coil) while decreasing the gas flow until the plasma could be sustained on vaporized material alone. The initially used charge material was a common nail. The mass spectrum which resulted was dominated by sulphur peaks. Replacing this by a rod of 99.98% pure iron resulted in a large Fe^+ mass peak and only a few minor contaminants which were rejected by the analyzer.

The intensity of the iron beam was roughly a factor of 3 lower than the typical argon beam. Lower efficiency at all stages is to be expected because of the heavier mass, which may account for the major part of the reduction. Detailed measurements of the iron beam properties and retardation have been prevented by problems with other parts of the apparatus.

2.3.5 Chopper Operational Tests

A prototype version of the electronic chopper shown in Figure 6 was tested using the center einzel electrode for beam modulation. The repelling potential applied was only 200 v, instead of the 540 v calculated. Nevertheless, the beam was completely stopped (or defocused) for the "off" portion of the cycle, and was transmitted as usual during the "on" phase. The beam signal did not faithfully reproduce the chopper output waveform, however, but instead exhibited rather slow and irregualr rise and fall times. This will not be a serious problem because of the detector arrangement to be used.

The final version of the chopper has been built, but has not yet been successfully operated due to component failure at high voltages. It is believed that the problems have been solved and that the unit will be successful in its next test.

3.0 COLLISION REGION FOR $Fe^+ \rightarrow N_2$ EXPERIMENTS

The first experiment to be performed will be a determination of the emission cross sections for Fe^+ impinging on an N_2 target at meteoric velocities. The preceeding section dealt with the production and control of the ion beam. In this section we shall discuss the target chamber, including its facilities to handle the target gas, measure the required parameters, and detect the radiation produced.

3.1 Mechanical Design of the Collision Chamber

Besides being a chamber to retain the target gas, the collision chamber incorporates the following features: an entrance slit to admit and collimate the beam, while minimizing gas effusion; a Faraday cup to measure ion beam intensity; a window to allow photons produced to be transmitted to a monochromator; an inlet valve for the target gas; a valved connection for a McLeod gauge; and electrical feedthroughs for the Faraday cup and other electrodes that will be required. Still to be added are a thermistor or other temperature-sensing device to measure gas temperature, a collector for charge-exchanged slow ions which will be produced, and optics to introduce light from a standard lamp for detector system calibration.

The collision chamber and its accessories were shown diagrammatically in Figure 1. The chamber consists of a 4" i.d., heavy wall aluminum tube inserted right through the experimental chamber vacuum housing, and having ports at both ends. A piece of copper shim, having an etched slit 1 mm x 10 mm, is clamped over a slot in the chamber wall to act as the beam aperture. The Faraday cup (to be described later) is mounted on teflon supports opposite the entrance slit. A 1 1/8 diameter viewing window is mounted on the top of the chamber, directly over the tube center and in line with the beam. Gas and electrical feedthroughs are mounted on the end ports, as will be the standard lamp window.

Certain modifications or additions may be required. For example, it may be necessary to install an ion beam collimator and/or an aperture in the optical path, to make the slits and Faraday cup moveable from outside the vacuum system, and to reduce the entrance slit size. Judgement will be reserved on these matters until more data are available.

3.2 Faraday Cup

The Faraday cup consists of three electrodes, insulated from each other and mounted on teflon rails. The rails are attached to the inside wall of the collision chamber. The cup assembly may be moved along the rails for alignment.

The first electrode is an aluminum plate with a 1/16" x 9/16" slot through which the beam passes. In operation, it is either grounded directly or through a microammeter. Its purpose is to measure the outer fringes of the beam, thereby establishing a geometrical limit on the interaction region. For absolute cross section measurements it is necessary that the primary ion beam current collected by this plate be much less than the total beam current. It is is not possible to achieve this condition by proper electrical focusing of the beam, it will be necessary to place an additional beam collimator before the interaction region.

The second electrode has a slightly larger slit (1/8" x 5/8") and serves the dual functions of mechanical spacer (1/4" thick) and secondary electron suppressor. It is shadowed from the ion beam by the first plate. It is normally biased a few volts negative to prevent secondary electrons from leaving the cup collector itself.

The cup collector is a closed volume except for its entrance aperture (3/16" x 3/4"). It is grounded through a microammeter and serves to measure the ion intensity.

An argon beam has been run through the apparatus and detected

by the cup. There was some loss in the maximum attainable beam current compared to that obtained with the detector array and shown in Figures 8 - 11. Of a total current of about 4 μA to all collectors of the cup, nearly 3 μA could be focused through the slit and into the main cup collector. More studies will be done to see if the entire beam can be directed into the cup without striking the entrance plate.

The characteristics when the beam was retarded were identical to those described earlier; i.e., there was little loss of total beam intensity down to a few hundred electron volts.

A variable negative voltage applied to the suppressor electrode was observed to have the expected effect. Below 1000 eV beam energy, little or no change in measured intensity resulted as the suppressor voltage was increased. Above this energy a slight decrease in current was observed, representing the suppression of secondary electrons, up to a maximum effect of 10% to 15% at the maximum attainable beam energy of 3 keV. Only 10 v to 15 v suppressor voltage was required to reach the current plateau.

3.3 Gas Handling System

A gas-handling system, including an auxiliary vacuum system, was built to control the gas flow to the collision chamber. It is shown schematically in Figure 13. The operation of the system is evident from the drawing. Two storage bulbs and valving manifolds are provided so a second gas can be supplied to the ion source or to a charge-exchange chamber, if such a procedure is necessary for future experiments. The McLeod gauge can be used to measure the pressure in the auxiliary system or in the target chamber.

3.4 Optical System Design

The system to measure the optical radiation produced in a collision may be divided into three basic units: fore-optics to collect and

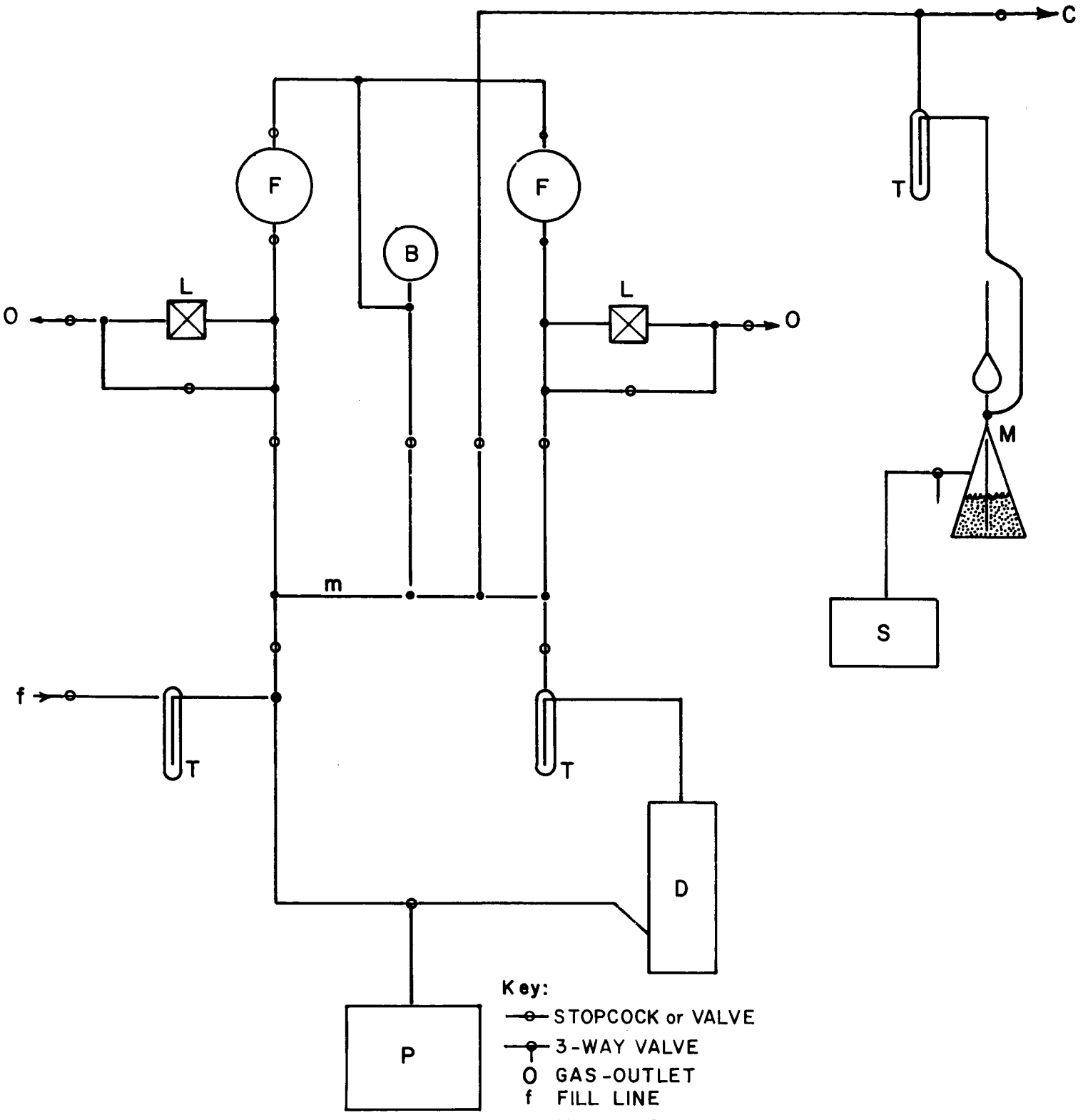

Figure 13 Gas Handling System

focus the light, a dispersing element to separate the spectral components, and a radiation detector.

3.4.1 Fore-Optics

The design of a light channeling system depends on the wavelength range desired, the particular dispersing device chosen, and the geometry of the apparatus. We here anticipate the selection of the disperser, which is a monochromator of optical speed f/5.3 and with slits adjustable up to 2 cm high by 2 mm wide. For best efficiency, the radiation should fill both the field-of-view of the monochromator and its entrance slit, which is equivalent to placing the entrance slit at the source of radiation. Neglecting transmission losses, no optical system can do better.

It is possible to increase the radiant flux by increasing the source brightness, however. Therefore, for the uniformly radiating volume shown in Figure 14, the useful photon flux through slit "A" is greater than for "B". This is just the geometry of our beam experiment. Since it is physically impossible to place the monochromator slit at the interaction region, its slit must be imaged there by a lens/mirror system, resulting in the layout shown in the figure. The 45° mirror is used to rotate the image so the monochromator can be mounted in its normal position, and the beam image is reduced by the lens so a narrower slit can be used to improve spectral resolution. The lens is large enough to fill the field-of-view, and the slit is just filled by the source image.

3.4.2 Dispersing Element

Aside from certain mechanical features and cost restrictions it was desired to choose a spectrum analyzer with the greatest possible wavelength range, optical efficiency, and field-of-view. The unit chosen was the McPherson Model 218, which is a high-efficiency, grating monochromator with an f/5.3 optical system and a scan range of 1050 Å to

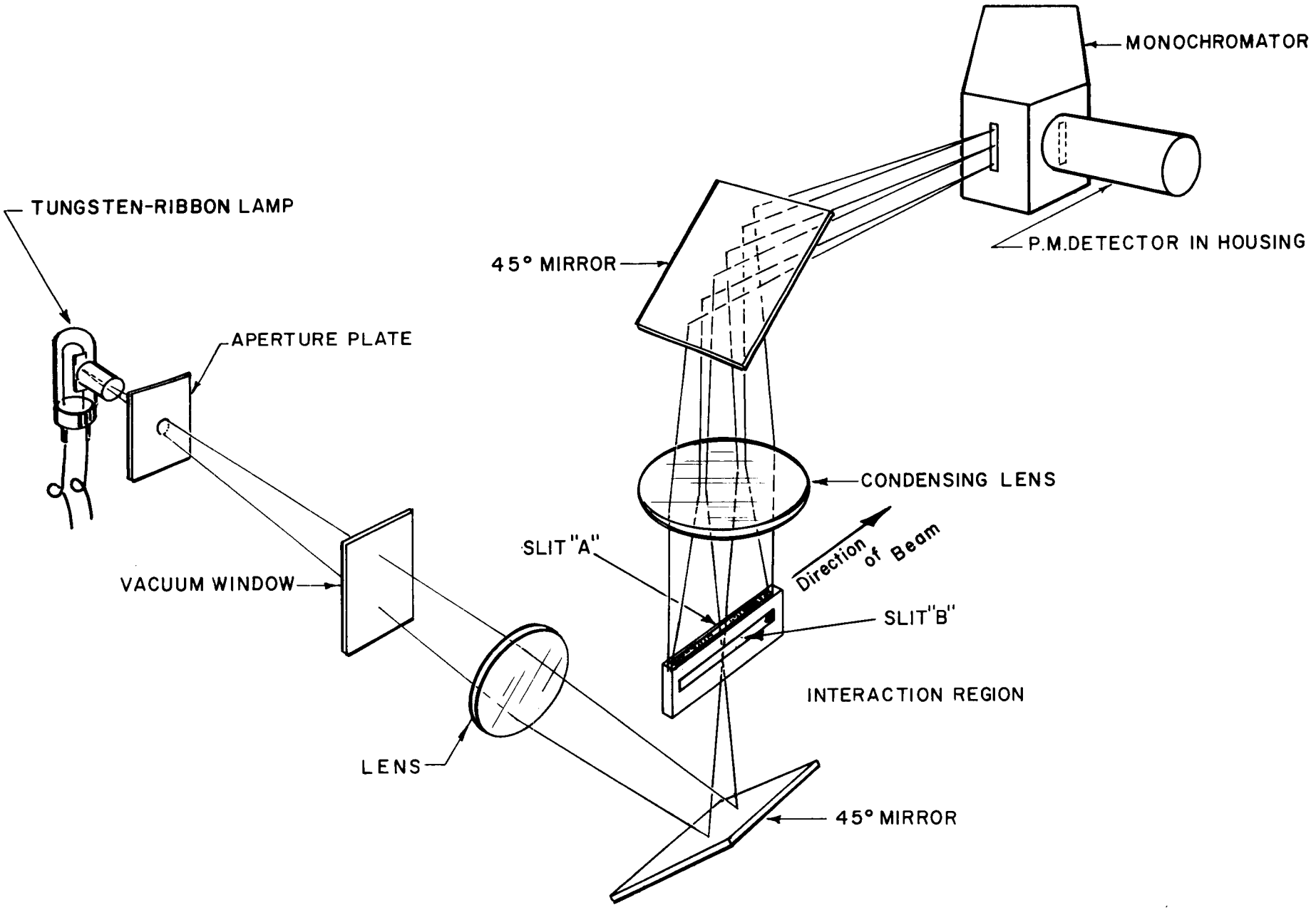

Figure 14 Optical Arrangement

1 μ with its standard grating. It also has the useful features of automatic scan, adjustable slits, and evacuable housing. Photomultiplier detectors may easily be added. The observable wavelengths are not limited by the monochromator, but by quartz optics and photomultiplier cathode response.

In order to make absolute measurements of the radiation intensity, we must have slits wide enough to transmit the entire image of the interaction region, or alternatively know exactly what fraction they are rejecting. In operation, the slits can be opened until no increase in signal is observed. For better spectral resolution they can be partially closed at the cost of introducing uncertainties in absolute intensities.

3.4.3 Radiation Detector

In accord with the monochromator specifications, a highly sensitive photon detector with a broad spectral response is required. Since the planned system is to count single photon pulses rather than measure aggregate currents (see Section 4) it is also desired that the detector have a high gain, fast transit times with little time spread, and a well-defined pulse height distribution for single photoelectrons. An Amperex 56 TUVP photomultiplier was the best choice of available tubes for the purpose. It has an "extended" S-20 cathode for UV response down to 1800 Å, and is useful to above 0.7 μ. For measurements from 0.7 μ to 1.0 μ a tube with S-1 cathode response will be required. The photomultiplier will be mounted directly on the monochromator exit flange in a coolable, shielded housing.

3.5 Optical Calibration

The optical system described above must be calibrated by comparison with a source of known spectral distribution and output, such that the calibration light passes through the same optical system as radiation from the collisional interaction region. A convenient and reliable source for

the range 2500 Å to several microns is a tungsten ribbon lamp of the type used as a radiance standard by the National Bureau of Standards.

When an aperture is placed as close as possible to the exit window of the lamp, it is approximately an f/50 system. In order to make this fill the field of the monochromator it is necessary to use a reducing lens to produce a more divergent beam passing through the collision region (the quantity known as spectral radiance, power per unit wavelength per unit area per steradian, is conserved). This situation is also shown in Figure 14. The calibration light will therefore appear to radiate from a point source located somewhere in the volume of the interaction region. It will be necessary to map the response from all parts of the interaction region and apply a correction to the observed signal to account for variations. For a well designed optical system with slight aberrations, the correction should be small.

Calibration for the region below 2500 Å is much more difficult. One possibility is to use a source which produces a series of spectral lines of known intensity ratios, and which are distributed in such a way that they may be used to extrapolate the system response to lower wavelengths. More work will be done to establish a calibration procedure for these lower wavelengths.

4.0 PROPOSED OPERATING PROCEDURE

In order to evaluate the emission cross sections versus energy for radiation produced by the ion-molecule collisions, it is necessary to have the following information pertaining to the interaction region:

1. ion energy,
2. number of incident ions,
3. path length under observation,
4. target density,
5. number of photons produced at a particular wavelength.

Of course we must also know the incident particle and target gas species; for this reason we included the mass analyzer and will use high-purity gases in the collision chamber.

Items 1, 3 and 4 above, as well as the observed wavelength, are established by the system parameters and geometry. Target gas density will be determined from the observed pressure and temperature in the collision chamber. The pressure will be measured by an electronic (capacitance) manometer, calibrated against the McLeod gauge using a non-condensible, inert gas such as helium (Reference 7). Thermocouples or thermistors mounted on the walls of the collision chamber will be used to measure the temperature. It remains to relate the Faraday cup and photomultiplier outputs to the numbers of incident ions and resulting photons respectively.

4.1 Detector Electronics

4.1.1 Photon Measurement

The problem of determining the number of photons produced at the interaction region breaks conveniently into two parts: (1) determination of the transfer function of the optical system up to the output of the photomultiplier and (2) processing of the photomultiplier output in a convenient way. The optical system and the calibration method, which will

yield the total transfer function, have already been discussed. We now consider how the photomultiplier output is to be handled.

We recall that the ion beam is to be chopped so that selective detection methods may be employed to separate the modulated signal from random noise and any d.c. background that may be present. Of several widely used detection techniques, all of which are phase-locked for good noise rejection, the use of a gated pulse-counting procedure appears to be most useful for our purposes (References 8 and 9). Our estimated photon arrival rates are low enough (see Section 4.2) to be well within the capabilities of fast counting circuits, so we can simply count the output pulses in one or the other of two scalers, depending on the modulation phase. It is also worthy of note that counting methods are less susceptible to noise pickup and zero drift than are other demodulation systems.

The procedure is to amplify the pulses, to remove the low-level noise pulses (of amplitude less than that corresponding to single photoelectrons) by threshold discrimination, and to count the discriminator output by dual scalers gated such that one records "beam off" counts, the other "beam on". One scaler will thus indicate signal plus background, the other background only, and randomly occurring noise pulses will have been averaged between them as part of the background. The signal is then given by the difference S, with a standard deviation $\sqrt{S + B}$. Most other lock-in detection methods filter out the d.c. background and noise so that information is lost.

Since the chopped ion beam has been observed to have poorly defined rise and fall-times, it would be useful to suppress data during those intervals and to accumulate counts only when the beam is completely "off". This is easily accomplished by proper control of the scaler gating pulses, and is a great advantage not available with other lock-in methods.

4.1.2 Ion Current Measurement

We wish to measure the ion beam intensity during the same time intervals for which the scalers are gated on. Two possible means are available to measure the beam "on" and beam "off" ion currents, while avoiding the irregular rise and fall times. The first is to simply use a calibrated oscilloscope to measure the desired part of the waveform as it appears across a precision resistor on the Faraday cup output. A second method, which has many advantages, is to use a gated voltage measuring device which samples only a selected portion of a repetitive waveform. An example of such a device is the Model CW-1 Boxcar Integrator manufactured by Princeton Applied Research Corporation.

When its time-base scan is triggered in phase with a repetitive signal applied to its input, the Boxcar Integrator can sample and average any part of the input waveform determined by a variable delay, variable width gate. (Long RC integration times may be used to recover the gated portion of the signal from high noise levels, if that situation occurs.) The major advantage of the instrument for our application, however, is that it can be used in an internal time-base mode, for which both time-base and gate outputs are available. It can therefore be used to generate our modulation rate and to gate the scalers, with very little auxiliary circuitry. We can then determine the number of ions (current x "on" time) and the number of photons (counts x transfer function) for identical time intervals, which is all the information we require.

4.2 Estimated Signal

It is informative to estimate the magnitude of the photon count rates we can expect. We have

$$R_\lambda = R_I \times \sigma_\lambda \times L \times n$$

where R_λ = numbers of photons produced per second at wavelength λ

R_I = number of incident ions per second

σ_λ = emission cross section for photon at wavelength λ

L = length of interaction region

n = target gas density

For our example, let us assume $R_I \sim 10^{13}$ particles per second (1 μ A), $\sigma_\lambda \sim 10^{-18}\,cm^2$, L = 1 cm, and the target gas pressure is 10^{-3} torr. Under these conditions we compute

$$R_\lambda \approx 3.5 \times 10^8 \text{ photons/sec.}$$

The number of counts per second at the scalers (neglecting background, which should be small), is given by $N = R_\lambda \times F$, where F is the optical system transfer function:

$$F \approx (\Omega / 4\pi) \times T \times Q$$

where Ω = solid angle collected by the optics,

T = transmission of the optics,

Q = quantum efficiency of the photocathode.

The geometry of the optical design gives $\Omega \approx 7 \times 10^{-3}$ steradians. We assume T ~ 100% and Q ~ 1%. Then we get for the count rate, $N \approx 2 \times 10^3$ pulses per second.

A similar calculation based on the geometry and the known spectral output of the standard lamp indicates that it will produce count rates exceeding 10^5 counts per second, even attenuating a factor of 10^3 with a neutral density filter. Since the photons would be emitted randomly, and would be distributed about the mean counting rate by a Poisson distribution, it is necessary to resolve counts some 100 times faster than the mean to achieve 1% accuracy in the calibration statistics. For this reason it will be necessary to have very fast pulse counting circuitry, such as is available from only a few sources.

5.0 PRESENT & FUTURE EFFORT

Most of what has been described in this report is pertinent to the experiments which will determine the emission cross sections for $Fe^+ \rightarrow N_2$ collisions. Iron beams have been run through the apparatus and detected at the Faraday cup, and a simple detector system has been set up to observe collisional excitation produced when the beam impinges on a gas leaked into the collision chamber. It is expected that these simple measurements will take place within the next couple of weeks, and will aid in "tuning up" the apparatus for measurements of the spectral features and emission cross sections.

Much of the major equipment needed has been ordered, and is already being received at AS&E. The capacitance monometer and fast counting equipment are still to be ordered, as are the photomultiplier base and housing and the calibration equipment. It is expected that several weeks will be required to set up the new equipment. There will undoubtedly be additional setup work necessary before the optical system and internal geometry of the collision chamber take final form. We expect that preliminary spectral data will be forthcoming by the end of June, and that the measurements of absolute cross sections will be under way by mid-summer.

Meanwhile, design studies will be started for the $N_2^+ \rightarrow Ca$ emission cross section experiments. They will utilize the same apparatus and optical system as the $Fe^+ \rightarrow N_2$ experiments, except that the collision region will be replaced by a calcium oven and detector. Most of the design effort will center about these items. No difficulty is anticipated in producing the beam, but a detector of known efficiency may be another matter.

6.0 REFERENCES

1. K. O. Nielsen, Nuclear Instruments 1, 289 (1957).
2. A. von Engel, Ionized Gases, Clarendon Press (Oxford, 1965).
3. J. E. Jordan and I. Amdur, Jour. Chem. Phys. 46, 165 (1967).
4. S. H. Neff, Thesis, Harvard University (1963).
5. C. R. Spangenberg, Vacuum Tubes, McGraw-Hill (1948).
6. P. Grivet, Electron Optics, Pergamon Press (1965).
7. N. G. Utterback & T. Griffity, Jr., Rev. Sci. Inst. 37, No. 7 (July, 1966).
8. R. R. Alfano and N. Ockman, Jour. Opt. Soc. of Am. 58, 90 (1968).
9. G. A. Morton, Applied Optics 7, 1 (1968).

7.0 APPENDIX

A New Technology report is to be submitted under separate cover by the AS&E New Technology Officer.